Chapter 3
Material Characterization

3.1 Introduction

The study of material characterization of FRP is very important for its application in construction. To understand the behavior of any materials or structures, it is essential to have complete description of the composition of materials and its properties. Accurate material characterization is essential for correct modelling and designing of a structure. For the design prospect, it is very important to determine the physical and mechanical properties of FRP beams. Because the composition of fiber and stiffness of beams varies, if it is produced by different manufacturers. Therefore, it is necessary to predict the material properties of FRP beams using suitable test methods. In this chapter, the experimental tests carried out for the prediction of strengths and stiffness of pultruded beams are presented. Moreover, analytical methods used to predict the Young's and shear moduli are discussed in detail.

3.2 Description of beams

This research is performed on the beams having perfect and imperfect geometries, i.e., without and with imperfection. In beams with imperfection, top flange is not perpendicular to the web as shown in Fig. 3.1(a), while in beams without imperfection, flanges are perpendicular to the web. Imperfection in the flange is 5.93% and is calculated as ratio of relative difference between the levels of the longitudinal edges of compression flange lying on each side of web. The beam without imperfection consists of same layup, type of fibers and resin as in beams having imperfection. These beams were manufactured by Agni Fiber Boards Pvt. Ltd., using pultrusion process. Beams with and without imperfection are denoted by 'PULT-A' and 'PULT-B', respectively. Dimensions of beams and stacking sequence of fibers in beams PULT-A and PULT-B are presented in Figs. 3.1(a) and (b), respectively. The stacking sequence of the beams was determined as per guidelines of ASTM standards (ASTM D2584, 2008), which is explained in the section 3.4.1. As it is observed that stacking sequence of the beams PULT-A and PULT-B is same, therefore material properties of both beams are same. Hence, in this thesis material properties of PULT-B beam are shown. In order to use pultruded beams in civil engineering applications, it is necessary to provide higher web-flange junction strength and transverse stiffness of panels, because failure of web-flange junction by crippling or crushing is the primary failure of I-sections. Therefore, layup of the beam PULT-B is modified (without changing the size of cross-section) to increase the transverse strength of web as well as increasing

the strength of web-flange junction. The beam having modified layup is denoted by 'PULT-C' and the stacking sequence is presented in Fig. 3.1(c). The number of CSM layers in the modified beam (PULT-C) are decreased from four to two and uni-directional rovings are added in 45° and 90° to the longitudinal axis of the beam. Moreover, the number of roving layers in 0 degree are increased from 3 to 4, which increases the elastic modulus and tensile strength of beam. The role of 45° and 90° laminae is to provide integrity to resist shear and make proper connection between flange and web elements. As per supplier, polyester resin was used in all beams. The grade of resin and hardener was 'Resin 691' and 'Reactive Polyamide 140', respectively.

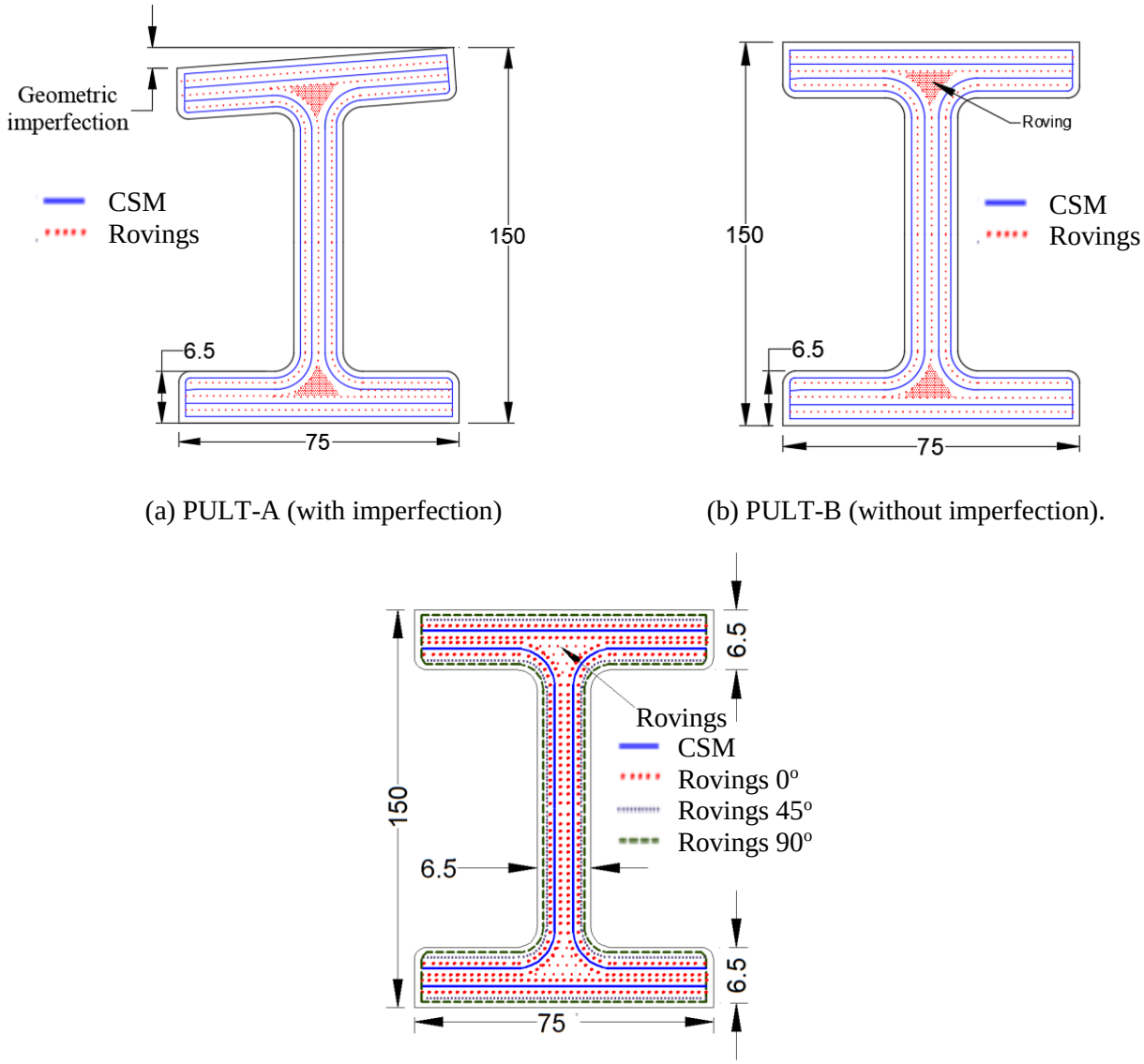

(a) PULT-A (with imperfection)

(b) PULT-B (without imperfection).

(c) PULT-C

Fig. 3.1. Dimensions and layup of I-beams.

(CSM is chopped strand mat)

3.3 Analytical method

In this section, an approach for determining the stiffness of the beam is presented using two theories, i.e., approximate Classical Lamination Theory (CLT) and Mechanics of Laminated Beams theory (MLB). Following sub sections provide the approach to evaluate the stiffness of lamina and beam.

3.3.1 Fiber volume fraction and stiffness of lamina

The stiffness of laminae is determined using methods such as rule of mixtures, periodic microstructure and composite cylinder model, and Manera method. Young's and shear moduli of each lamina are derived from rule of mixtures while shear modulus is derived from periodic microstructure and composite cylinder model. Manera method is followed to determine the stiffness of CSM layer. Using rule of mixtures (Jones, 1975), the longitudinal (E_1) and transverse (E_2, i.e., stiffness along the width of the laminate) moduli of roving and stitched fabrics is determined using Eqs. (3.1) and (3.2), respectively.

$$E_1 = E_f V_f + E_m V_m \tag{3.1}$$

$$E_2 = \frac{E_f E_m}{E_f V_m + E_m V_f} \tag{3.2}$$

where, E_f is the Young's modulus of fiber, E_m is the Young's modulus of matrix and V_f is the fiber volume fraction of fibers in a lamina. The fiber volume fraction of the stitched fabrics is determined using Eq. (3.3).

$$V_f = \frac{w_u}{\rho t} \tag{3.3}$$

where, w_u is the unit weight of the lamina (i.e. weight/Area); ρ is the density of lamina and t is the thickness of the lamina. The fiber volume fraction of lamina of rovings (Davalos et al., 1996) can be computed from below equation:

$$V_f = \frac{n_r A_r}{t_r} \tag{3.4}$$

where, n_r is the number of roving per unit width, A_r is the area of one roving and t_r is the thickness of roving layer in pultruded beam. This thickness is calculated by subtracting the thickness of all others layers from the thickness of panel (flange and web) of I-section. Area of roving (A_r) is obtained from Eq. (3.5).

$$A_r = \frac{1}{\gamma \rho} \tag{3.5}$$

where, γ is the yield of the fiber, i.e., the length of fiber in 1 gram. Using rule of mixtures, shear modulus of a lamina is determined from Eq. (3.6).

$$G_{12} = \frac{G_f G_m}{G_f V_m + G_m V_f} \tag{3.6}$$

where, G_f and G_m are the shear moduli of fibers and the matrix, respectively. The stiffness of continuous strand mat (CSM), i.e., random oriented short fibers is determined based on Manera method (Ning, 1996). Elastic and shear moduli of CSM layer are determined as

$$E = V_f \left(\frac{16}{45} E_f + 2E_m \right) + \frac{8}{9} E_m \tag{3.6}$$

$$G = V_f \left(\frac{2}{15} E_f + \frac{3}{4} E_m \right) + \frac{1}{3} E_m \tag{3.7}$$

where, V_f is the fiber volume fraction of laminate which is determined from Eq. (3.3). Based on Periodic microstructure theory (Luciano and Barbero, 1994), the expression of shear modulus is given as

$$G_{12} = G_m - V_f \left[-\frac{S_3}{G_m} + \frac{1}{G_m - G_f} \right]^{-1} \tag{3.8}$$

where, S_3 is computed by:

$$S_3 = 0.49247 - 0.47603 V_f - 0.2748 V_f^2 \tag{3.9}$$

The equation of shear modulus of any lamina based on composite cylinder model (Hashin and Rosen, 1964) is given by:

$$G_{12} = G_m \frac{\left(1+V_f\right) G_f + \left(1-V_f\right) G_m}{\left(1-V_f\right) G_f + (1+V_f) G_m} \tag{3.10}$$

The calculated value of stiffness of each lamina is presented in Table 3.1.

Table 3.1 Properties of plies of beams.

Beam	Lamina	Thickness (mm)	V_f	Rule of mixture (ROM)			MM♠		PM♣	CM♦
				E_1 (GPa)	E_2 (GPa)	G_{12} (GPa)	E (GPa)	G_{12} (GPa)	G_{12} (GPa)	G_{12} (GPa)
PULT-A & PULT-B	CSM	0.45	0.38	28.21	27.30	2.00	13.26	2.03	2.58	1.57
	Roving¥	1.58	0.36	26.39	3.43	1.74	-	-	2.13	1.49
PULT-C	CSM	0.35	0.55	39.47	39.47	2.69	14.81	6.85	4.53	4.49
	Roving¥	1.24	0.45	33.00	4.01	2.69	-	-	3.17	3.16
	Stitched*	0.42	0.57	40.96	5.34	2.81	-	-	4.00	3.98

*0° and 90° fibers rovings (orientation is w.r.t. longitudinal axis) are stitched, ¥ Fiber orientation is 0° along the axis of the beam, ♠ Manera method, ♣ Periodic microstructure, ♦ Composite cylinder model.

3.3.2 Stiffness of beam

Details of approximate classical lamination and mechanics of laminated beam theories for predicting the overall stiffness of beam is given in the following sections:

3.3.2.1 Approximate classical lamination theory

The stiffness of the beam can be calculated by measuring the stiffness of lamina of flanges and web and then combining together to obtain the stiffness of pultruded I-beam. Nagaraj and Gangarao (1997) derived the approximate isotropic modulus of flanges and web including the effect of stiffness of fiber in transverse direction. Therefore, this theory is known as approximate classical lamination theory (CLT). An approximate isotropic modulus of a lamina is given by

$$E_r = Q_{11} - \frac{Q_{12}^2}{Q_{22}},\ Q_{11} = \frac{E_1}{1-\nu_{12}\nu_{21}},\ Q_{22} = \frac{E_2}{1-\nu_{12}\nu_{21}} \text{ and } Q_{12} = \nu_{12}Q_{22} \tag{3.11}$$

Based on this theory, extensional stiffness of flanges is calculated using Eq. (3.12)

$$A_f = b_f \sum_{r=1}^{N} E_r t_r \tag{3.12}$$

where b_f is the width of the flange, while E_r and t_r are the approximate modulus and thickness of the r^{th} lamina, respectively. Similarly, bending stiffness matrix of flange and web is computed using Eqs. (3.13) and (3.14), respectively.

$$D_f = b_f \sum_{r=1}^{N} E_r \left[t_r Z_r^2 + \frac{t_r^3}{12} \right] \tag{3.13}$$

$$D_w = \frac{h_w^3}{12} \sum_{r=1}^{N} E_r t_r \tag{3.14}$$

where, h_w is the depth of web. Overall bending stiffness of a beam is calculated by combining the stiffness of each panel, i.e., web and flanges and is given by Eq. (3.15),

$$D_y = D_f + A_f z^2 + D_w \tag{3.15}$$

where, z is the distance between center of flange and centroid of the cross-section. Shear modulus of beam is computed by addition of shear stiffness of each layer of the web. Shear rigidity of flanges is neglected. Shear rigidity of web (F_w) is given below:

$$F_w = h_w \sum_{r=1}^{N} G_r t_r \tag{3.16}$$

where, G_r is the shear stiffness of rth lamina of the web.

3.3.2.2 Mechanics of laminated beam theory

This method considers the effect of coupling induced in the beam due to un-symmetrical layup of beam. The compliance matrix of each panel of beam is determined using classical lamination theory. Stiffness of each panel can be calculated from the following equations:

$$A_i^{'} = \left(\delta_{11}\Delta^{-1}\right)_i,\ B_i^{'} = \left(\beta_{11}\Delta^{-1}\right)_i,\ D_i^{'} = \left(\alpha_{11}\Delta^{-1}\right)_i,\ F_i^{'} = \left(\alpha_{66}^{-1}\right)_i \text{ and } \Delta = \alpha_{11}\delta_{11} - \beta_{11}^2 \tag{3.17}$$

where, $[\alpha] = [A]^{-1}$, $[\beta] = [B]^{-1}$ and $[\delta] = [D]^{-1}$ and A_i is extensional stiffness, B_i is bending-extension coupling stiffness, D_i is bending stiffness of a laminate and subscript 'i' denotes the panel number. These [A], [B] and [D] stiffness matrices are calculated by classical lamination theory. While $A_i^{`}$, $B_i^{`}$, $D_i^{`}$ and $F_i^{`}$ are the stiffness of a panel considering the effect of coupling. Total extensional stiffness of the FRP beam considering the effect of local stiffness of the panels is given by:

$$A_x = \sum_{i=1}^{n} A_i^{'} b_i \tag{3.18}$$

where, b_i is the width of panel and n denotes the number of panels. The reference axes of the beam are considered at the centroid of cross-section, i.e., at the center of the web. The depth of neutral axis of beam is represented by z_n and is calculated using Eq. (3.19),

$$z_n = \frac{\sum_{i=1}^{n}\left(z_i A_i^{'} + \cos\theta_i B_i^{'}\right) b_i}{A_x} \tag{3.19}$$

where, z_i is distance between center of the panel and the centroid of the beam and 'θ' is the angle between the axis of panel and Y-axis of the beam. The co-ordinate system of the beam followed for stiffness calculations is shown in Fig. 3.2. The equation to evaluate bending-extension (B_y), flexural rigidity (D_y), and shear rigidity (F_z) of beam are given as

$$B_y = \sum_{i=1}^{n} A_i^{'}\left[A_i^{'}\left(z_i - z_n\right) + B_i^{'}\cos\theta_i\right] b_i$$

$$D_y = \sum_{i=1}^{n}\left[A_i^{'}\left(\left(z_i - z_n\right)^2 + \frac{b_i^2}{12}\sin^2\theta_i\right) + 2B_i^{'}\left(z_i - z_n\right)\cos\theta_i + D_i^{'}\cos^2\theta_i\right] b_i$$

$$F_z = \sum_{i=1}^{n} F_i b_i \sin^2\theta_i \tag{3.20}$$

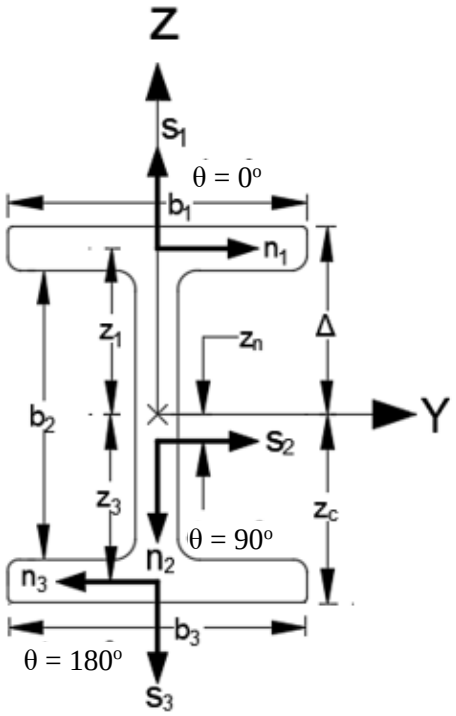

Fig. 3.2. Coordinate system of FRP I-beam.

Based on above two theories, stiffness of each panel and beams are presented in the Table 3.2. It is observed that Young's and shear moduli obtained using approximate CLT and MLB are close. Young's modulus of CSM layer is calculated using Manera method, it is because Young's modulus predicted from rule-of-mixtures is very high, but in actual its value is low (as per the manufacturer properties). The Young's modulus of other layers (rovings and stitched fabrics) is calculated using rule of mixtures as well as shear modulus of each layer is predicted from rule of mixtures. Using rule of mixtures and Manera method (for calculation of Young's modulus of CSM) in approximate CLT and MLB theories, analytical results are closer to experimental results, which is explained in the preceding section (3.5).

Table 3.2 Stiffness (GPa) of beams obtained by approximate CLT and MLB theories.

Beam	**Stiffness Parameter**	**Approx. CLT**	**MLB**
PULT-A & -B	E	22.62	22.77
	G	1.96	1.97
PULT-C	E	27.81	27.95
	G	2.38	2.38

3.4 Experimental investigation

In order to measure the properties of beams, coupons were cut on Power hack saw machine in the workshop at BITS-Pilani, followed by grinding the edges of coupons, to remove the extra fibers and maintaining the required shape of coupons. Different sizes of coupons were cut as per the recommendation of codes such as ASTM D2584 (2008), ASTM D3039 (2014), ASTM D3410 (2008) and ASTM D790 (2002). Samples were prepared for tensile, compressive, flexural, and shear testing. The coupons were cut from interior area of flanges and web of pultruded I-beam. The junction of flange and web was avoided for coupons due to non-uniformity of fiber. Moreover, edges of flanges were also avoided because of broken edges and irregularities in thickness. For each test, five coupons were cut, and specimen's ID based on test and origin of specimen from beams are presented in Table 3.3. The first letter of each specimen ID denotes the name of test, like 'T' stands for tension testing, 'C' stands for compression testing, 'S' stands for shear testing, 'F' stands for flexural testing of coupons, while the second letter denotes the name of beam, i.e., 'B' represents beam PULT-B and 'C' denotes beam PULT-C. The last letter 'F' or 'W' represents the origin of the specimen, i.e., specimen taken from flange or web of the beam, respectively. The composition of the fiber in pultruded beams was measured by ignition of samples as per ASTM D2584 (2008). Young's modulus was obtained through tension test as described in ASTM D3039 (2014). Compressive strength of

specimens was measured as per specifications recommended by ASTM D3410 (2008), while ASTM D790 (2002) specifies the procedure for calculation of flexural modulus of FRP beams and coupons by 3-point bending test.

Table 3.3 Description of specimens for different tests.

Specimen ID	Type of test	Origin of the specimen	Specimen ID	Type of test	Origin of the specimen
TBF	Tensile test	Flange of PULT-B	SBF	Short beam test♦	Flange of PULT-B
TCF	Tensile test	Flange of PULT-C	SCF	Short beam test	Flange of PULT-C
TBW	Tensile test	Web of PULT-B	SBW	Short beam test	Web of PULT-B
TCW	Tensile test	Web of PULT-C	SCW	Short beam test	Web of PULT-C
CBF	Compression test	Flange of PULT-B	FBF	Flexural test♣	Flange of PULT-B
CCF	Compression test	Flange of PULT-C	FCF	Flexural test	Flange of PULT-C
CBW	Compression test	Web of PULT-B	FBW	Flexural test	Web of PULT-B
CCW	Compression test	Web of PULT-C	FCW	Flexural test	Web of PULT-C

♦Interlaminar shear test, ♣Three-point bending test of coupons

3.4.1 Physical and mechanical properties of specimens

The physical and mechanical properties of specimens obtained using different tests are described in the following sections:

3.4.1.1 Fiber content

The composition of the fiber in pultruded beams was measured by ignition of samples as per the method suggested by ASTM D2584 (2008). FRP specimens of size of 25 x 25 x 6.5 mm were extruded from the web and flanges of beams. Samples were kept in muffle furnace at 550^{o}C for half an hour as shown in Fig. 3.3. Ignition loss of resin content was determined by weighing the specimen before and after igniting. Using ASTM D2584 (2008) resin content was determined by Eq. (3.21)

$$\text{Resin content} = \text{Percentage of weight loss} = \frac{(W_1 - W_2)}{W_1} \times 100 \tag{3.21}$$

where, W_1 and W_2 represents the weight of specimen and residue, respectively. From the above method, percentage of resin content in flanges and web of beams PULT-A and PULT-B is 29%, while the corresponding values for beam PULT-C is 26%. The layer of each fabric was separated out from the burnt coupons of both beams. From the physical observation, it seen that, fiber is not uniform specially at edges

of flanges. Therefore, coupon should not be extruded from the edges of flange. The layer-wise description of the beams is shown in Fig. 3.1.

(a) Before burning (b) Aftter burning

Fig. 3.3. Ignition of samples in a muffle furnace for removal of resin.

3.4.1.2 Tensile characteristics

To predict the mechanical properties such as Young's modulus, tensile strength and Poisson's ratio, tensile tests were performed as per ASTM D3039 (2014). Five rectangular coupons of approximate size 250 x 25 x 6.5 mm were extruded from PULT-B and PULT-C beams. The tension tests were conducted on a universal testing machine of 100 kN capacity. Rate of displacement of cross-head was 2 mm/min. The coupon was inserted in between the pressure wedge grips at both ends and pressure of 6.89 MPa was set in grips. With this pressure, there was no slippage and breakage of the specimen inside the grips. While placing the specimen inside the grips, it was ensured that coupons are perfectly straight.

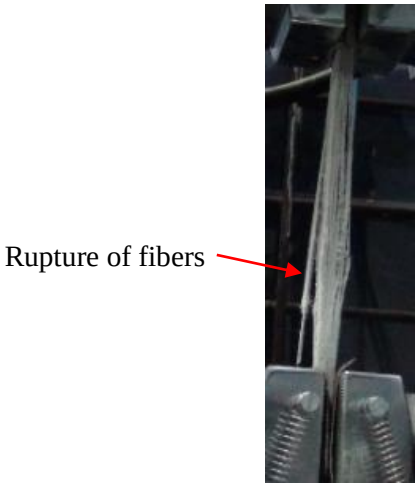

Fig. 3.4. Tensile testing of coupon.

The failure of the samples was sudden and the sound produced was like a gunshot and the failure was in the form of delamination of continuous strand mat and cracking of rovings in longitudinal as well as transverse directions. The stress-strain curves obtained from tensile test of beams PULT-B and PULT-C are shown in Figs. 3.5(a) and 3.5(b), respectively. Fig. 3.5(a) shows that stress-strain curves of specimen of beam PULT-B obtained from tensile test is linear till failure. From Fig. 3.5(b), it is noted that all tensile specimens of beam PULT-C show bi-linear stress-strain behavior. The Young's modulus was calculated from the first linear portion of stress-strain curve. The Young's modulus of coupons of the web and flanges of PULT-C is much closer due to the same fiber volume fraction in flanges and web.

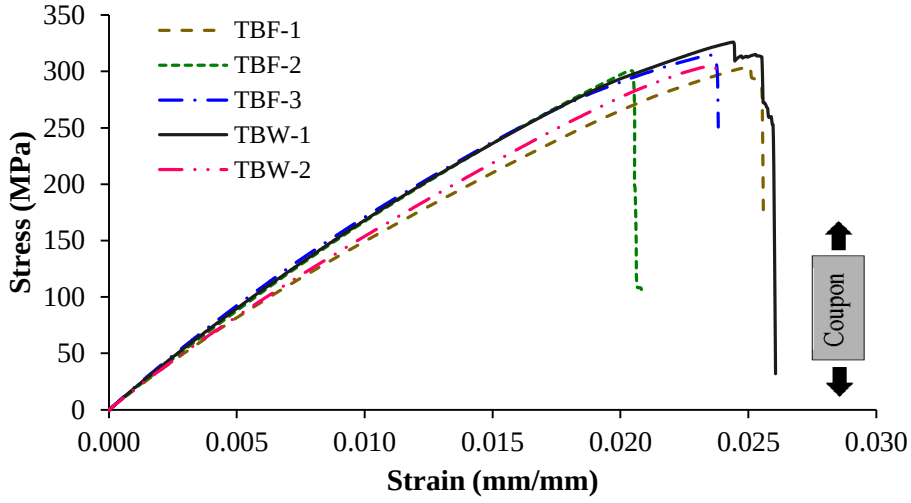

(a) Beam PULT-B

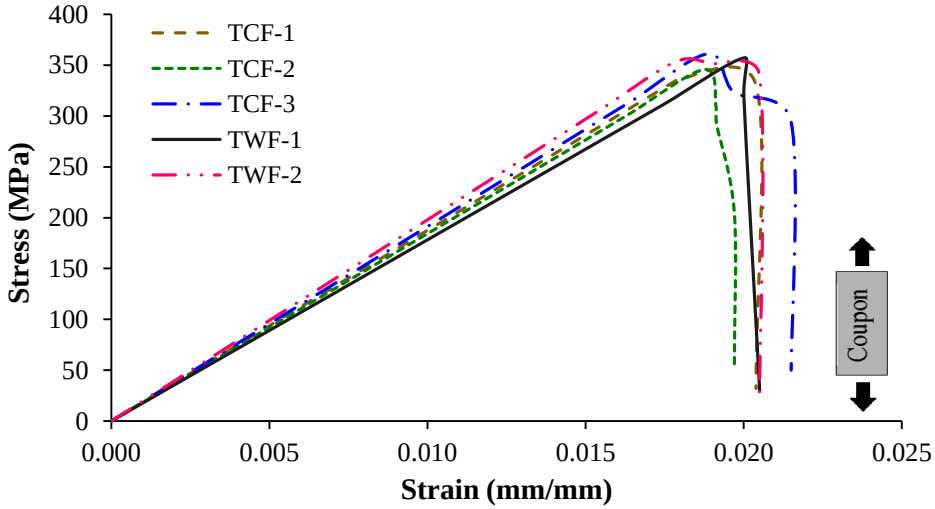

(b) Beam PULT-C

Fig. 3.5. Stress vs strain curves obtained from tensile testing of coupons.

Table 3.4 Tensile characteristics of pultruded FRP beams PULT-B and PULT-C.

Specimen Id	Young's modulus (GPa)	Tensile strength (MPa)
TBF-1	16.25	303.93
TBF-2	16.25	300.49
TBF-3	16.25	314.87
TBW-1	13.58	325.98
TBW-2	14.88	303.67
TCF-1	18.75	335.74
TCF-2	18.43	345.81
TCF-3	19.12	361.00
TWF-1	17.82	357.21
TWF-2	19.79	353.04

3.4.1.3 Compressive characteristics

The compressive strength of the specimen of pultruded beams was measured as per the guidelines given in ASTM D3410 (2008). Five specimens each of sizes 125 x 25 x 6.5 mm (length x width x thickness) were extruded from each beam. Test was performed under displacement control mode with a constant rate of movement of cross head as 1.5 mm/min. In this way, incremental compressive load was applied until specimen failed. Fig. 3.6 shows the mode of failure of specimen in compression. After the failure of a specimen, it was noted that all specimens failed by delamination (see Fig. 3.6) of fabric layers, which is consistent with the failure mechanism reported by Correia (2012). Due to high stress concentration near the grip, external layer got folded as well as delamination occurred in the between the layers. In Table 3.5, compressive strengths of coupons from flanges and web of PULT-B and PULT-C beams are presented.

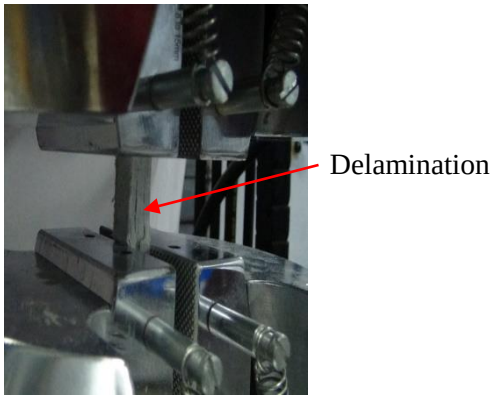

Fig. 3.6. Compression testing of specimen.

Table 3.5 Compressive strength of the specimens.

Specimen ID	Compressive strength (MPa)	Transverse compressive strength (MPa)*
CBF-1	246	44.59
CBF-2	267	48.41
CBF-3	241	45.74
CBW-1	253	43.46
CBW-2	259	45.59
CCF-1	334	59.15
CCF-2	344	57.25
CCF-3	324	56.28
CCW-1	397	60.98
CCW-2	384	59.06

*Specimens were cut along the depth of the beam

3.4.1.4 Flexural modulus from 3-point bending test of FRP coupon

The ASTM D790 (2002) specifications were used to measure the stiffness of FRP coupons. The coupons of approximate size 360 x 15 mm (length x width) were extruded from the FRP beam, with L/d ratio of 60, for minimizing the effect of shear. A special fixture was self-fabricated and attached to the bottom head of actuator with loading nose of 12 mm diameter and sample was placed on the supports of 6 mm diameter as shown in Fig. 3.7. The test was continued until the complete specimen failure, i.e., visible delamination and cracks in ply (or flaw) occurred under the loading. Tests were conducted under displacement control mode, with rate of displacement (R) 0.5 mm/s. Using ASTM D790 (2002), the displacement rate was calculated using Eq. (3.23)

$$R = \frac{ZL^2}{6d} \tag{3.23}$$

where, L is the span length (mm), Z is the rate of straining of outer fiber, mm/mm and is equals to 0.01 (ASTM D790, 2002), and d is the depth (mm) of coupon. Flexural responses of coupons of beams PULT-B and PULT-C under 3-point bending are shown in Figs. 3.8(a) and 3.8(b), respectively. The variation in slope of the curves is due to different widths of coupons obtained during cutting.

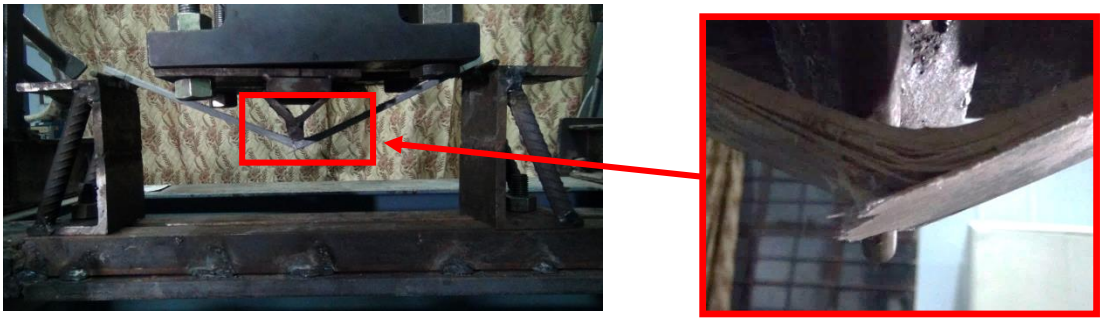

Fig. 3.7. Three-point bending test of coupon.

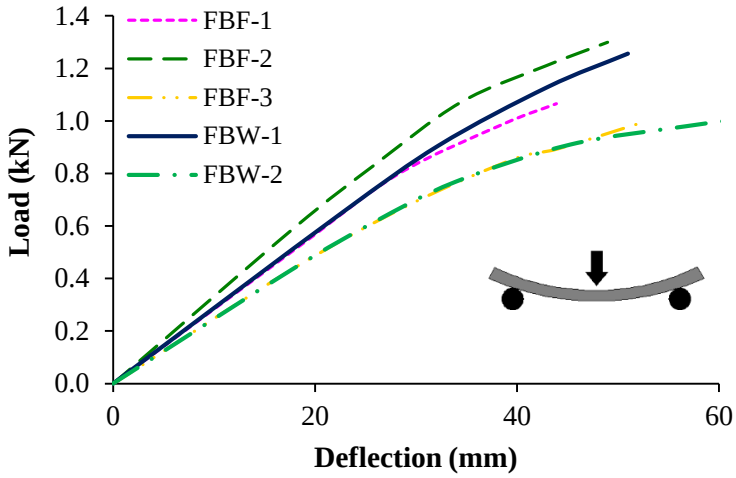

(a) Beam PULT-B

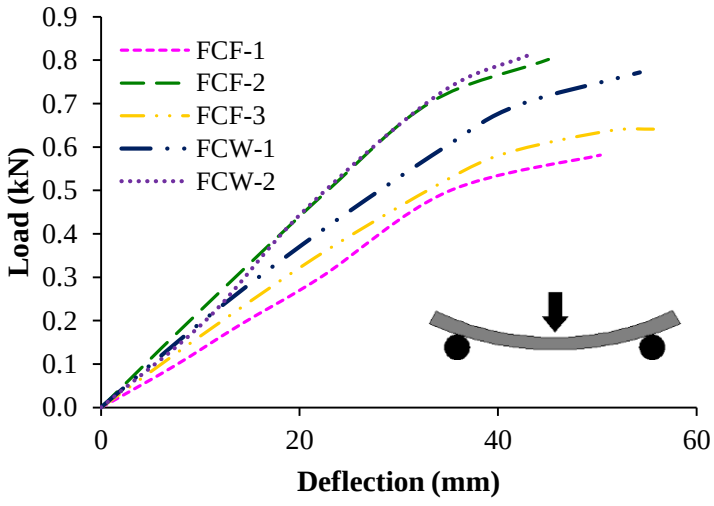

(b) Beam PULT-C

Fig. 3.8. Load versus deflection curves obtained from 3-point bending test of coupons of beams.

Table 3.6 represents the flexural modulus and strength of coupons obtained by three-point bending test. Flexural modulus was determined by measuring the slope of an initial linear portion of the curve and flexural strength was determined from the maximum bending moment and section modulus. The flexural modulus (E, GPa) of a specimen measured from 3-point bending test is given by

$$E = \frac{L^3 m}{4bd^3} \tag{3.24}$$

where, L (mm) is the span length; m (kN/mm) is the slope of the initial linear portion, b (mm) is width of specimen and d (mm) is the depth of the specimen. Modulus of elasticity of PULT-C, calculated from three-point bending test is nearly similar to results of tensile testing, while the modulus of elasticity of beam PULT-B is significantly different from that obtained from uniaxial tensile test. It is because misalignment of fibers in the coupons during fabrication of beams by pultrusion process.

Table 3.6 Flexural modulus and strength obtained from 3-point bending test of coupons.

Specimen ID	**Flexural modulus (GPa)**	**Flexural strength (MPa)**
FBF-1	19.34	284.75
FBF-2	21.14	323.07
FBF-3	18.48	290.83
FBW-1	21.34	320.03
FBW-2	23.54	321.33
FCF-1	21.36	287.22
FCF-2	26.87	372.10
FCF-3	20.19	302.83
FCW-1	22.19	378.16
FCW-2	22.57	364.22

3.4.1.5 Interlaminar shear strength

To determine the interlaminar shear strength of the specimen, short beam tests were performed as per ASTM D2344 (2000). Short beams specimens were cut from beams PULT-B and PULT-C in sizes of 40 x15 x 6.5 mm. Span length-to-depth ratio was maintained 4 during testing. Overhang on each support was kept equal to thickness of specimens. The test set-up of short beam shear test is shown in Fig. 3.9(a). The beam was loaded until the interlaminar crack appears in the thickness of coupon as shown in Fig. 3.9(b). This figure shows the failed specimen under flexural loading with interlaminar shear crack through the

thickness of specimen. Using ASTM D2344 (2000), shear strength of specimens was determined by Eq. (3.25).

$$\sigma_S = \frac{0.75P}{bh} \tag{3.25}$$

where, P is the maximum load, b is the width and h is the thickness of the specimen. The interlaminar shear strength of coupons are presented in Table 3.7. It is observed that the coupons of both beams PULT-B and PULT-C have almost same shear strength, for flanges and web. There is little variation in strength of coupons of PULT-B, due to the misalignment of fiber in flanges and web.

(a) Short beam shear test of coupon

(b) Interlaminar shear failure of the specimen

Fig. 3.9. Response of short span coupon under flexural loading.

Table 3.7 Interlaminar shear strength of coupons.

Specimen ID	Shear strength (MPa)
SBF-1	46.57
SBF-2	45.82
SBF-3	50.19
SBW-1	47.58
SBW-2	47.32
SCF-1	61.48
SCF-2	65.16
SCF-3	64.94
SCW-1	59.79
SCW-2	61.52

3.4.1.6 Mechanical properties using bending test of beams

(a) Experimental setup

In order to test the beams with simply supported boundary conditions, torsional restraints were provided at the supports to resist the rotation as well as translation of the beam. A special fixture was fabricated in the workshop at BITS-Pilani to provide the translation as well as torsional restraints to beams. Hence, in order to test the beams of different sizes, restraints kept movable on the fixture. They are connected to the fixture with bolts and nuts, so as to adjust the distance between them as per the size of beams. Beams were allowed to bend in the plane of loading only; therefore, out-of-plane displacement of the beam was restrained by providing the torsional restraint near to the application of the load as shown in Fig. 3.10. Friction between the surface of restraints and beam was reduced through a thin film of grease. An LVDT was installed laterally under the loading to measure the lateral deflection of beams and another LVDT was used to measure the vertical displacement of the beam. In order to reduce the stress concentration at the load application, load was applied through the bearing plates, similarly bearing plates were provided upon supports to reduce the stress concentration on the joint of flange and web. The load and deflections were recorded with frequency of 30 Hz and saved in the personal computer.

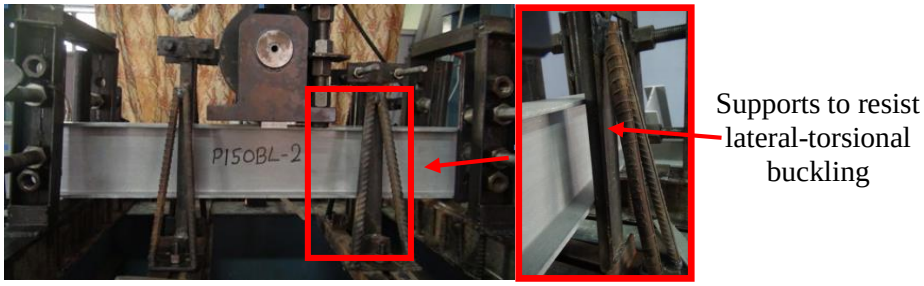

(a) Three-point bending test

(b) Four-point bending test

Fig. 3.10. Flexural testing of beams.

(b) Three-point bending test of profiles

The maximum deflection of a beam due to flexure and shear under 3-point bending can be measured using the following equation (Reddy, 2003):

$$w = \frac{PL^3}{48EI_y} + \frac{PL}{4GK_zA} \tag{3.26}$$

where, w is the deflection at mid-span, P is applied load, L is the distance between the supports, E is the flexural modulus, I_y is the moment of inertia of beam about y-axis, G is the shear modulus, A is the area of section and K_z is shear coefficient and is taken as 5/6 (Roberts and Ubaidi, 2002). Eq. (3.26) can be re-written as

$$\frac{4Aw}{PL} = \frac{1}{12E}\left(\frac{L}{r}\right)^2 + \frac{1}{GK_z} \tag{3.27}$$

The above equation represents the equation of a line. Flexural modulus can be calculated from 3-point bending test of I-beams with different values of $\left(\frac{L}{r}\right)^2$. The slope of graph between $\frac{4Aw}{PL}$and $\left(\frac{L}{r}\right)^2$ can be used to measure the flexural modulus (E) of I-beam. Hence, flexural modulus of a beam is given by Eq. (3.28),

$$E = \frac{1}{12 \times \text{Slope}} \tag{3.28}$$

On the other hand, the shear modulus is given by Eq. (3.29),

$$G = \frac{1}{K_z \times \text{inercept}} \tag{3.29}$$

Test program

In this test program, 3-point bending test was conducted on full-length of the pultruded beams. The $\left(\frac{L}{r}\right)^2$ ratio as measure of slenderness was taken as 100, 200, 300 and 400. Based on these slenderness ratios, PULT-B beams were cut into length of 0.40, 0.65, 0.80 and 0.95 m; while PULT-C beams were cut into 0.75, 1.0, 1.15 and 1.35 m. Overhang on each support was kept equal to half of the depth of section. Load was applied at the mid-span of simply supported beam and was statically increased until deflection reaches to maximum deflection of L/350. Long beams were tested with lateral-torsional restraints at supports and near the mid span (see Fig. 3.10) for preventing deflection in lateral direction, i.e. lateral-torsional buckling. A graph is plotted between $\frac{4Aw}{PL}$and $\left(\frac{L}{r}\right)^2$ up to the load of 1500 N (see Fig. 3.11). Young's modulus is calculated using Eq. (3.28) by measuring the slope of this graph. Similarly, shear modulus is determined from Eq. (3.29) after evaluating the intercept of the graph. The Young's modulus of beams PULT-B and

PULT-C is observed to be 15.72 GPa and 22.52 GPa, respectively. The shear modulus of beams PULT-B and PULT-C is 1.05 GPa and 2.10 GPa, respectively. The intercept values as shown in Fig. 3.11, for beams PULT-B and PULT-C are 1.1356, and 0.5703, respectively.

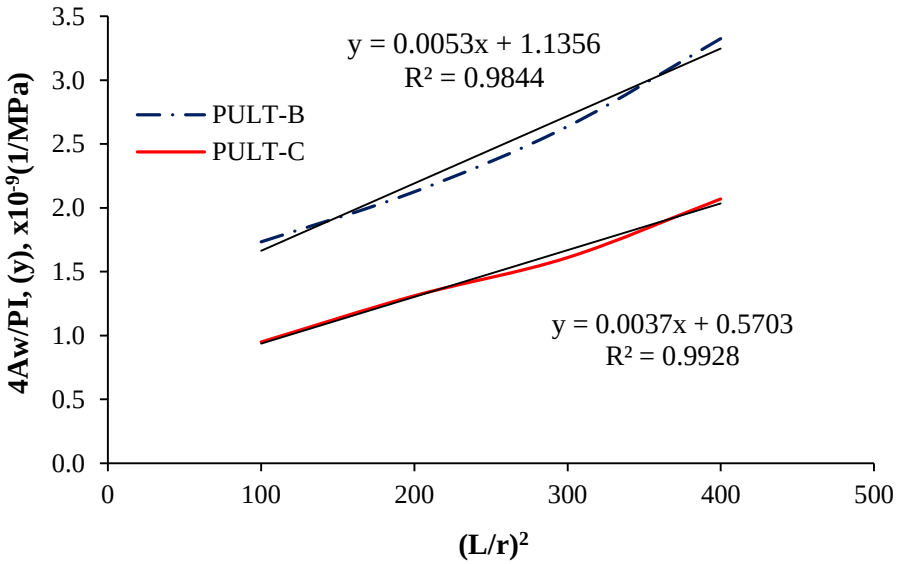

Fig. 3.11. Regression analysis of beams for measurement of Young's and shear moduli.

(c) Four-point bending test of beams

In this test program, supports were provided in between the loading, and the stiffness of beam is predicted as per the method prescribed by Minghini et. al. (2014), while the beams were loaded at ends as shown in Fig. 3.10(b). The main objective of providing loading at ends is to find the Young's modulus of the beam based on the pure bending of the beams, because in between the supports there is no shear deformation. Moreover, to find the shear modulus, span length between the end load and support is taken (i.e., cantilever portion), because the L/d ratio of cantilever portion is very low in comparison with span length in between the supports. As per availability of lengths, beams PULT-B and PULT-C were tested for the length of 1.9 and 2.1 m, respectively. Supports were provided under the beams (PULT-B and PULT-C) at end distance of L/6. Wooden stiffeners were provided in between flanges, to restrain the warping and torsion of beam about longitudinal axis. Vertical deflections were measured at the ends and mid-span of the beam. Responses of beams PULT-B and PULT-C are shown in Figs. 3.12(a) and (b), respectively. The flexural and shear rigidities of beam are determined using Timoshenko's beam theory (Reddy, 2003). The rigidities of the beam are given by following Eqs. (3.30) and (3.31).

$$EI_y = -Pa' \frac{\left(L - 2a'\right)^2}{8w_2} \tag{3.30}$$

$$K_Z GA = \frac{Pa'}{w_1 + \mu w_2} \text{ and } \mu = \frac{4a'\left(3L - 4a'\right)}{3\left(L - 2a'\right)^2} \tag{3.31}$$

where, P is the applied load at each end, w_2 is the vertical deflection of the beam at mid-span, w_1 is the vertical deflection at beam ends located at distance a' from supports and L is the distance between the supports. Deflections corresponding to the total load of 9 kN (i.e., 4.5 kN on each end) is used to determine the elastic properties of the beam. The Young's modulus of PULT-B and PULT-C beams is observed to be 21.13 and 26.98 GPa, respectively. The shear modulus of beams PULT-B and PULT-C is 2.18 and 2.42 GPa, respectively.

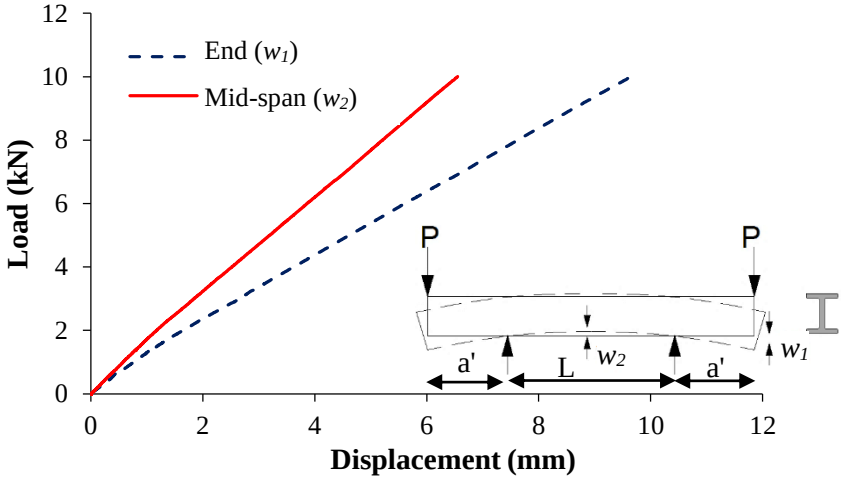

(a) Beam PULT-B

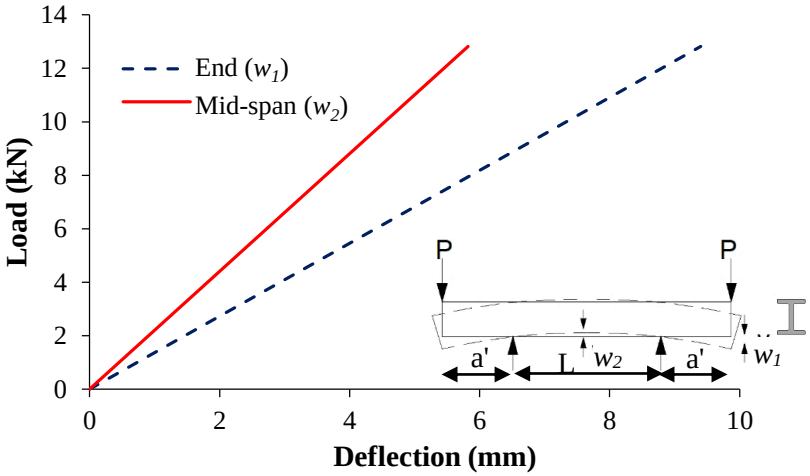

(b) Beam PULT-C

Fig. 3.12. Load-deflection responses of beams under four-point loading.

3.5 Results and discussion

Young's and shear moduli obtained from the various experimental tests and analytical methods are presented in Table 3.8. It is observed that Young's and shear moduli obtained using 3-point and 4-point beam bending tests are significantly different. This is because Young's modulus determined from 4-point beam bending test is based on pure bending of the beams (without shear deformation), i.e., simply supported span in between the supports, while in the 3-point bending test Young's modulus is obtained from equation which contains both Young's and shear moduli. In four-point bending test, L/d ratio is very low for prediction of shear modulus, while in three-point bending test it is high and the deflection equation used is couple with Young's modulus. Hence, there is difference in Young's and shear moduli obtained from both three-point and four-point bending tests. The difference in Young's modulus obtained from coupon and beam bending tests is due to the non-homogeneity and different orientation of fibers in the coupons. From Table 3.8, it is also observed that Young's and shear moduli obtained from theories are closer to that of the 4-point bending test of beams. The strengths and stiffness of the flanges and web are same, so averaged value of property of flange and web is determined and is presented in Table 3.8.

Table 3.8 Stiffness (GPa) of beams from analytical and experimental methods.

Beam	**Stiffness Param-eter**	**CLT♣**	**MLB♠**	**Tensile testing of coupons♦**	**3-point bending test of coupons***	**3-point bending test of beams**	**4-point bending test of beams**
PULT-A & -B	E	22.81	22.77	15.56	20.78	15.72	21.13
	G	1.97	1.97	-	-	1.05	2.18
PULT-C	E	28.03	27.95	20.23	21.05	22.52	26.98
	G	2.38	2.38	-	-	2.10	2.42

♣Approximate classical lamination theory, ♠Mechanics of laminated beam theory, *Average values of flexural modulus, ♦Average values of elastic modulus.

In order to check the accuracy of stiffness obtained from different analytical and experimental methods, load versus deflection responses are determined for a particular dimension of the beam using Eq. (3.26) with Young's modulus predicted from tensile testing of coupons, flexural testing of coupons, and beams, while the shear modulus is taken from four-point bending test because shear modulus is not predicted from these tests. The flexural responses obtained using Eq. (3.26) are compared with flexural response obtained from three-point bending test of same dimensions of the beam. It is noted that load-deflection response obtained from approximate CLT, MLB and 4-point bending test is closer to that obtained from experimental

testing of beam. Hence, it is concluded that stiffnesses obtained from 4-point bending test and theories are more accurate than those obtained from other tests.

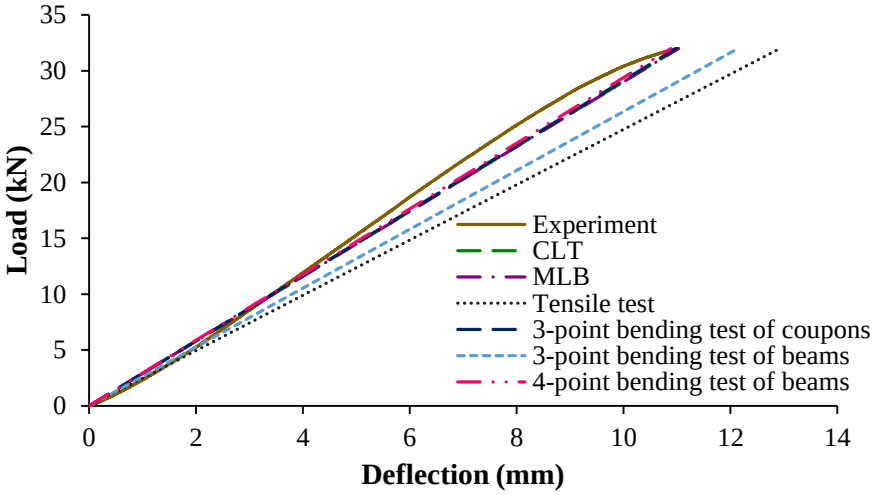

(a) Beam PULT-B

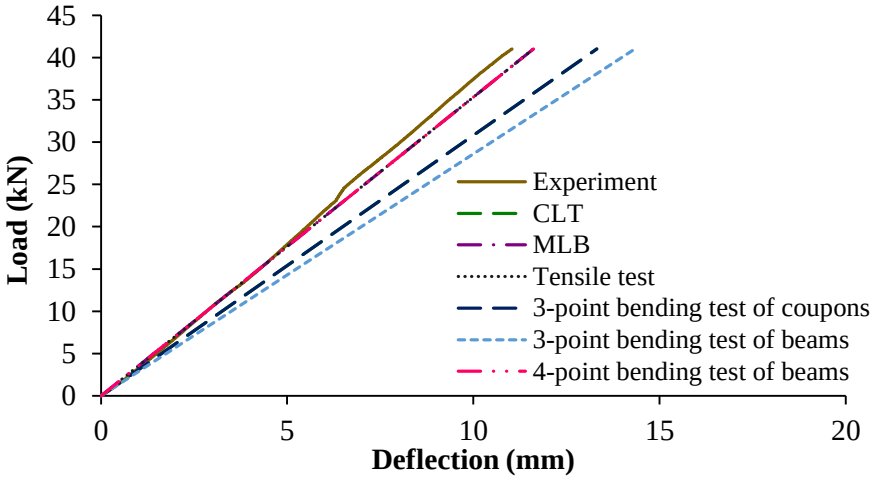

(b) Beam PULT-C

Fig. 3.13. Comparison of load-deflection responses obtained from experimental investigation and analytical Eq. (3.26).

Stifffnesses obtained from MLB consider the effect of coupling in calculation of stiffnesses of the beam, so this method is followed for further parametric study of FRP I-beams having different geometric and material properties (Chapter 6). Material properties of beams given in Table 3.9 are used to model the FRP beams with stiffening element in self-developed code in MATLAB and in FEM software ABAQUS. In this study, carbon fiber laminates are used as a stiffening element, which is explained in Chapter 6. Tensile properties of stiffening elements are determined by tensile testing of coupons (ASTM D3039, 2014), compressive properties are predicted by compression testing of coupons ASTM D3410, 2008) and shear

strength is determined by short shear test (ASTM D2344, 2000). The mechanical properties of carbon fiber laminates are listed in Table 3.9.

Table 3.9 Mechanical properties of beams and stiffening elements.

Properties	Beams PULT-A & PULT-B	Beam PULT-C	Carbon fiber laminate (CL)	Stiffening elements♣
Longitudinal modulus, E_1 (GPa)	22.77	27.95	41	30.12
Transverse modulus, E_2 (GPa)*	5.60	8.00	6.13	9.36
Shear modulus, G_{12} (GPa)	1.97	2.38	3.52	2.72
Poisson's ratio, v_{12}	0.28	0.28	0.27	0.28
Longitudinal compressive strength, (MPa)	253	356	653	360
Transverse compressive strength (MPa)	46	58	109	62
Shear strength, (MPa)	48	63	71	66

*Transverse tensile modulus and strength are determined by tensile testing of laminate having fiber orientation transverse to the longitudinal direction. ♣Angle shaped bearing stiffeners, cover plate, cover angle and web plate. Material properties of T-shaped bearing stiffener is similar to PULT-C

3.6 Conclusions

In this chapter, material characterization of pultruded beams is presented. It involves the measurement of resin content, tensile, compressive, flexural, and shear characteristics. Various methods were adopted for measurement for complete material characterization of FRP beams. The results obtained from experimental tests are verified with mechanics of laminated beam theory and approximate classical lamination theory. From this study, the following concluding remarks can be made:

1. Composition of fiber plays a vital role in prediction of elastic properties of pultruded FRP beams using analytical approach/theory.
2. Young's and shear moduli determined from the mechanics of laminated beam (MLB) theory and approximated laminated beam theory are in close agreement.
3. Young's modulus obtained from the rule of mixtures and Manera method, and the shear modulus obtained from rule of mixtures gives the good correlation between the 4-point bending test results and analytical results.
4. Stiffness determined from tensile and three-point bending testing of coupons, is highly affected by the location from where specimens were taken. Due to non-uniformity of fiber, coupons are not to be taken from the junction of flange and web, and the edges of flanges should also be avoided because of broken edges and irregularities in thickness.

5. The Young's and shear moduli determined from 4-point bending test are more accurate than that obtained from three-point bending test.